# Supporting Information

## Cyanophenyl spiro[acridine-9,9′-fluorene]s as simple structured hybridized local and charge-transfer-based ultra-deep blue emitters for highly efficient non-doped electroluminescent devices (CIEy ≤ 0.05)

Taweesak Sudyoadsuk,[a] Sujinda Petdee,[a] Chokchai Kaiyasuan,[a] Chaiyon Chaiwai,[a] Praweena Wongkaew,[b] Supawadee Namuangruk,[c] Pongsakorn Chasing[a] and Vinich Promarak*[ab]

[a] *Department of Materials Science and Engineering, School of Molecular Science and Engineering, Vidyasirimedhi Institute of Science and Technology, Wangchan, Rayong 21210, Thailand.*
*E-mail: vinich.p@vistec.ac.th*
[b] *Research Network of NANOTEC-VISTEC on Nanotechnology for Energy, Vidyasirimedhi Institute of Science and Technology, Wangchan, Rayong, 21210, Thailand.*
[c] *National Nanotechnology Center (NANOTEC), National Science and Technology Development Agency, Pathum Thani 12120, Thailand*

---

### 1. Material Synthesis

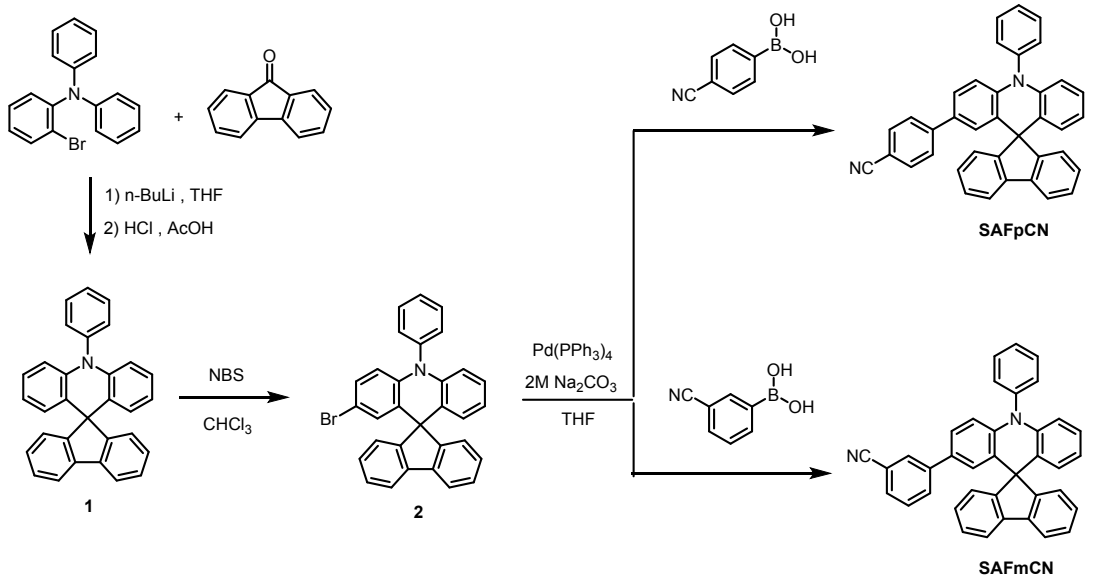


**Scheme S1**

***10-Phenyl-10H-spiro[acridine-9,9′-fluorene] (1)***

A solution of 2-bromotriphenylamine (3.22 g. 9.95 mmol) in THF (80 ml) in 250 ml three-necked round bottom flask was degassed with $N_2$ for 5 min. The solution was cooled to -78 °C for 30 min, and then 1.6M n-Butyl lithium in hexane (9.40 ml, 14.9330 mmol) was added dropwise via syringe. The resulting mixture was allowed to stir at -78 °C for 1 h, and then a solution of 9-fluorenone (1.79 g, 9.95 mmol) in THF (80 ml) was slowly added via additional funnel for 30 min. After 1 h reaction at -78 °C, for 1 h, the reaction mixture was warmed up to room temperature and stirred overnight. Water (20 ml) was added to the reaction mixture and THF was evaporated by rotary evaporator. The resulting mixture was extracted with DCM, washed with water and brine solution, dried over

anhydrous $Na_2SO_4$ and removed organic solvent, respectively. The light yellow crude product was dissolved in acetic acid (50 ml) and 37% HCl (5 ml) and then refluxed for 4 h. After cooling to room temperature, the precipitate was filtrated and washed with hexane. The resulting solid was purified by silica gel column chromatography using hexane as eluent to obtain a white solid (2.70 g, 67%). $^1$H NMR (600 MHz, $CDCl_3$) δ 7.80 (d, *J* = 7.5 Hz, 2H), 7.71 (t, *J* = 7.4 Hz, 2H), 7.58 (t, *J* = 7.3 Hz, 1H), 7.51 (d, *J* = 7.4 Hz, 2H), 7.44 (d, *J* = 7.4 Hz, 2H), 7.38 (t, *J* = 7.3 Hz, 2H), 7.26 (t, *J* = 7.2 Hz, 2H), 6.92 (t, *J* = 7.6 Hz, 2H), 6.56 (t, *J* = 7.3 Hz, 2H), 6.41 (d, *J* = 7.6 Hz, 2H), 6.36 (d, *J* = 8.3 Hz, 2H). $^{13}$C NMR (151 MHz, $CDCl_3$) δ 156.62, 141.37, 141.17, 139.25, 131.24, 131.07, 128.45, 128.38, 127.76, 127.58, 127.19, 125.82, 124.85, 120.55, 119.88, 114.64, 56.89. MALDI-TOF m/z $[M]^+$ calcd for $C_{31}H_{21}N$ 407.1674, found 407.3410.

***2-Bromo-10-phenyl-10H-spiro[acridine-9,9'-fluorene] (2)***

A solution of N-bromosuccinimide (0.087 g, 0.49 mmol) in chloroform (10 ml) was added dropwise to a solution of **1** (0.20 g, 0.49 mmol) in chloroform (20 ml). The mixture was stirred at room temperature for 1 h and then water (50 ml) was added. The mixture was extracted with DCM, washed with water and brine, dried over anhydrous $Na_2SO_4$ and removed organic solvent, respectively. The crude product was purified by recrystallization from DCM/Methanol mixture solvent to give a white solid (0.21 g, 88%). $^1$H NMR (600 MHz, $CDCl_3$) δ 7.81 (d, *J* = 7.5 Hz, 2H), 7.72 (t, *J* = 7.8 Hz, 2H), 7.59 (t, *J* = 7.4 Hz, 1H), 7.48 (dd, *J* = 8.3, 1.1 Hz, 2H), 7.42 – 7.39 (m, 4H), 7.28 (td, *J* = 7.6, 0.9 Hz, 2H), 6.99 (dd, *J* = 8.9, 2.3 Hz, 1H), 6.92 (ddd, *J* = 8.5, 7.2, 1.5 Hz, 1H), 6.58 (td, *J* = 7.4, 1.0 Hz, 1H), 6.49 (d, *J* = 2.3 Hz, 1H), 6.38 (dd, *J* = 7.8, 1.4 Hz, 1H), 6.35 (d, *J* = 8.4 Hz, 1H), 6.24 (d, *J* = 8.9 Hz, 1H). $^{13}$C NMR (151 MHz, $CDCl_3$) δ 155.84, 140.93, 140.74, 140.61, 139.18, 131.22, 130.96, 130.11, 130.06, 128.71, 128.52, 127.90, 127.65, 127.36, 127.01, 125.68, 124.66, 120.94, 120.10, 116.37, 114.73, 112.66, 56.64. MALDI-TOF m/z $[M]^+$ calcd for $C_{31}H_{20}BrN$ 485.0779, found 485.2946.

## 2. Characterization data

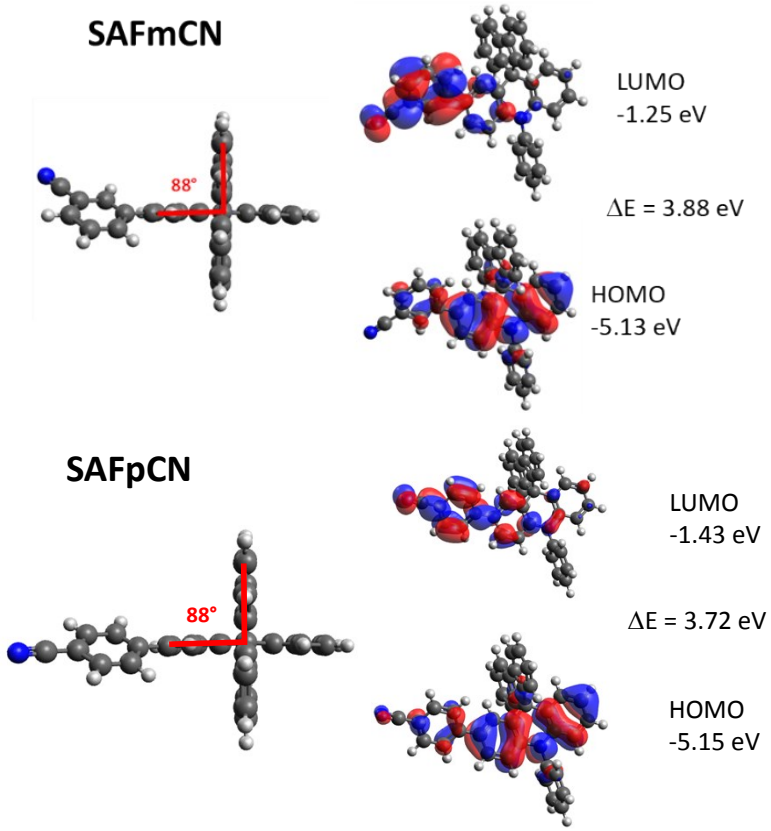


**Fig. S1** Optimized structures, and molecular orbital energy level and HOMO-LUMO energy gaps calculated by B3LYP/6-31G(d,p) function.

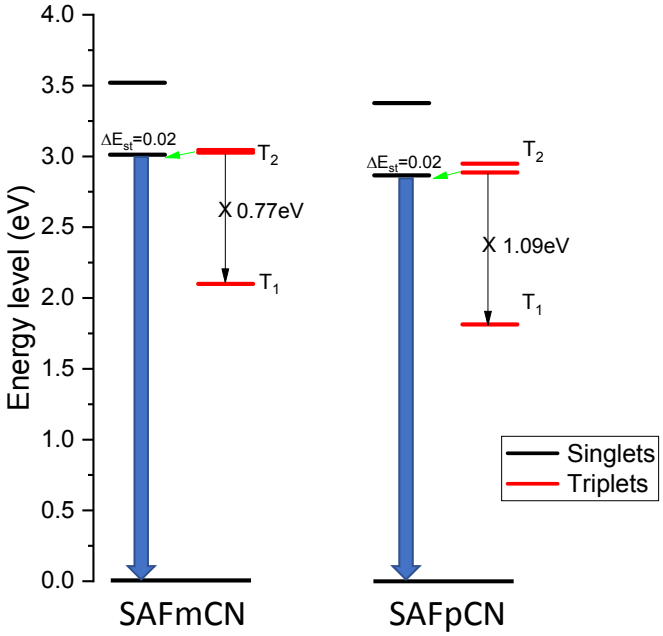


**Fig. S2** The energy diagram of singlet and triplet excited states of the compounds from TD-B3LYP/6-31G(d,p) calculations.

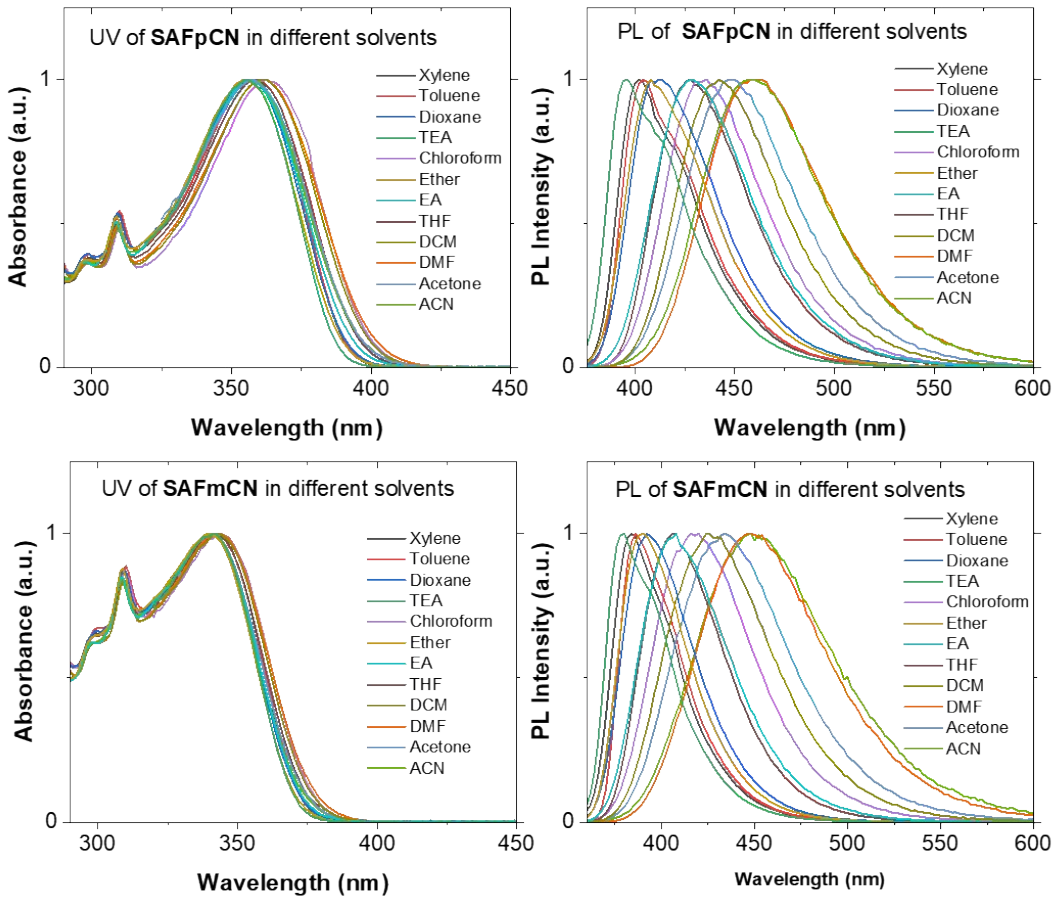


**Fig. S3** UV-vis absorption and PL spectra in different solvents.

**Table S1** Detail of the optical data in different solvents.

| Solvents | $\varepsilon$ | n | f($\varepsilon$,n) | SAFpCN | | | SAFmCN | | |
|---|---|---|---|---|---|---|---|---|---|
| | | | | $\lambda_a$ (nm) | $\lambda_f$ (nm) | $\upsilon_a$ - $\upsilon_f$ ($cm^{-1}$) | $\lambda_a$ (nm) | $\lambda_f$ (nm) | $\upsilon_a$ - $\upsilon_f$ ($cm^{-1}$) |
| Xylene | 2.57 | 1.496 | 0.003 | 358 | 402 | 3057 | 343 | 384 | 3113 |
| Toluene | 2.38 | 1.494 | 0.015 | 357 | 404 | 3259 | 343 | 386 | 3248 |
| Dioxane | 2.22 | 1.422 | 0.021 | 356 | 410 | 3700 | 340 | 394 | 4031 |
| Triethylamine | 2.42 | 1.401 | 0.048 | 355 | 396 | 2916 | 341 | 378 | 2870 |
| Chloroform | 4.81 | 1.446 | 0.148 | 363 | 434 | 4507 | 344 | 418 | 5146 |
| Ethyl ether | 4.34 | 1.352 | 0.167 | 355 | 408 | 3659 | 340 | 390 | 3771 |
| Ethyl acetate | 6.02 | 1.372 | 0.200 | 356 | 428 | 4725 | 340 | 408 | 4902 |
| Tetrahydrofuran | 7.58 | 1.407 | 0.210 | 359 | 428 | 4491 | 341 | 406 | 4695 |
| Dichloromethane | 8.93 | 1.424 | 0.217 | 361 | 442 | 5076 | 343 | 427 | 5735 |
| Dimethyl formamide | 37.0 | 1.427 | 0.274 | 361 | 460 | 5962 | 342 | 448 | 6918 |
| Acetone | 20.7 | 1.359 | 0.284 | 357 | 448 | 5690 | 340 | 434 | 6370 |
| Acetonitrile | 37.5 | 1.344 | 0.305 | 356 | 458 | 6256 | 340 | 450 | 7190 |

The dipole moment of ground state $\mu_g$ can be estimated by DFT calculation, and the the dipole moment of excited state are determined from the slope of linear fitted Stokes' shift ($\nu_a$-$\nu_f$) against orientation polarizability f(ε,n) in different solvents according to Lippert-Mataga equation.[1]

$$hc(\upsilon_a - \upsilon_f) = hc(\upsilon_a^0 - \upsilon_f^0) + \frac{2(\mu_e - \mu_g)^2}{a_0^3} f(\varepsilon, n),$$

$$f(\varepsilon, n) = \frac{\varepsilon - 1}{2\varepsilon + 1} + \frac{n^2 - 1}{2n^2 + 1},$$

Among which ε and n are dielectric constant and refractive index of solvent respectively, and $a_0$ is the solvent cavity radius

$$a_0 = (\frac{3M}{4N\pi d})^{1/3},$$

where N is Avogadro number, M is molecular weight, and d is density. Two-region trends found in **mTAHPI**, **pTAHPI** and **pTAPI** are steady slopes of 4774, 5099, and 4854 for low-polar solvents and sharp slopes of 21838, 23295, and 23477 for high-polar solvents.

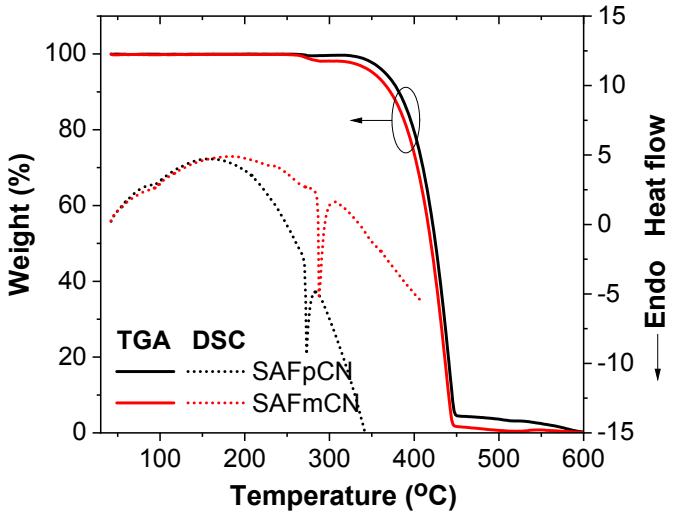


**Fig. S4** TGA and DSC (2nd heating scan) thermograms measured at heating rate of 10 °C min$^{-1}$ under $N_2$ flow.

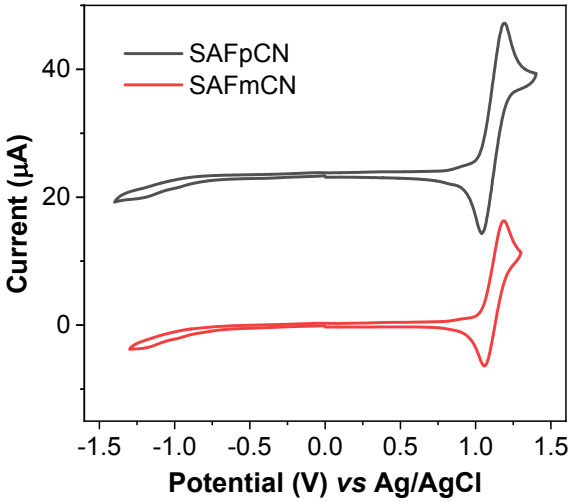


**Fig. S5** CV traces measured in $CH_2Cl_2$ containing n-$Bu_4NPF_6$ as a supporting electrolyte at a scan rate of 50 mV $s^{-1}$ under Ar atmosphere.

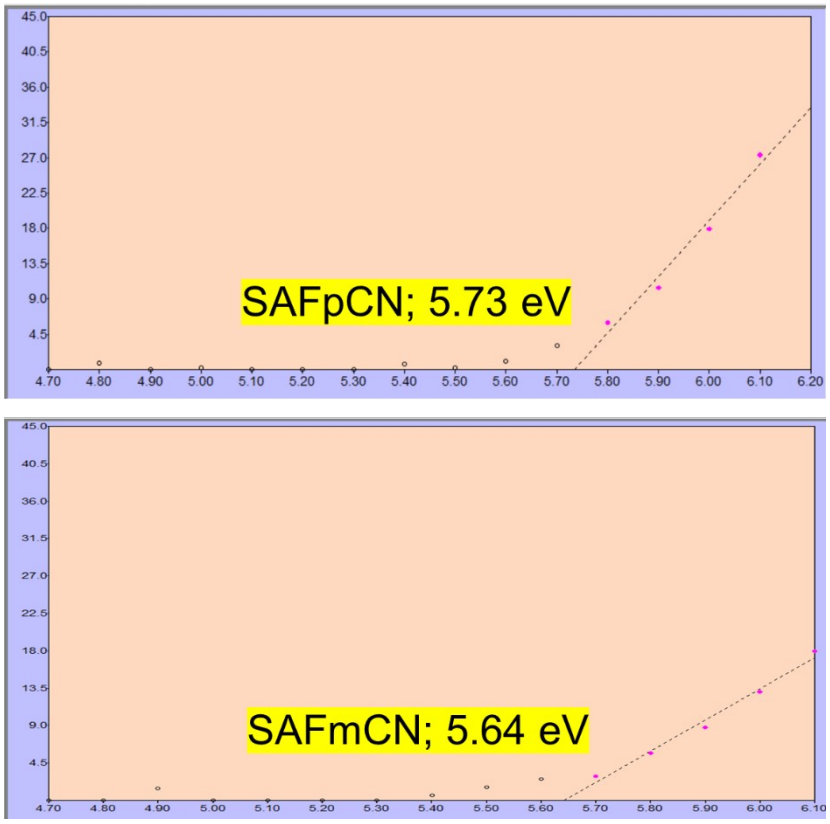


**Fig. S6** Photoemission yield spectroscopy in air (PYSA) spectra.

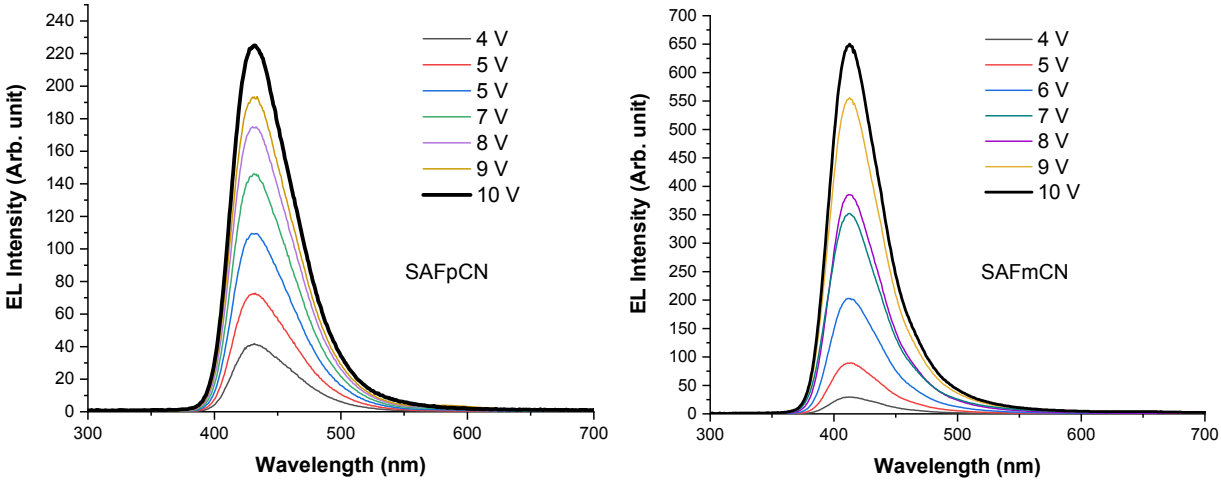


**Fig. S7** EL spectra of the fabricated OLEDs at different applied voltages.

## Reference

1) C. Feng, J. Li, X. Han, X. He, L. Liu, X. Li, X. Sun, P. Lu and Y. Ma, *Faraday Discuss.* 2017, **196**, 163-176.

**Fig. S8** Copy of NMR and HRMS MALDI-TOF spectra

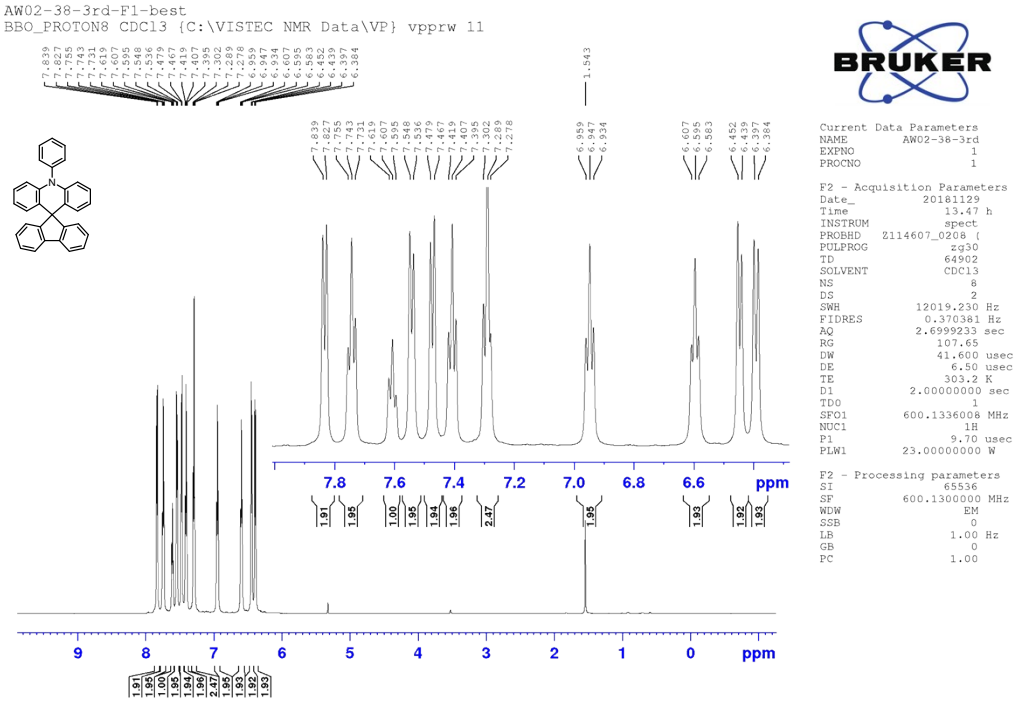


The $^{1}$H NMR spectra of **1** in $CDCl_3$ solution.

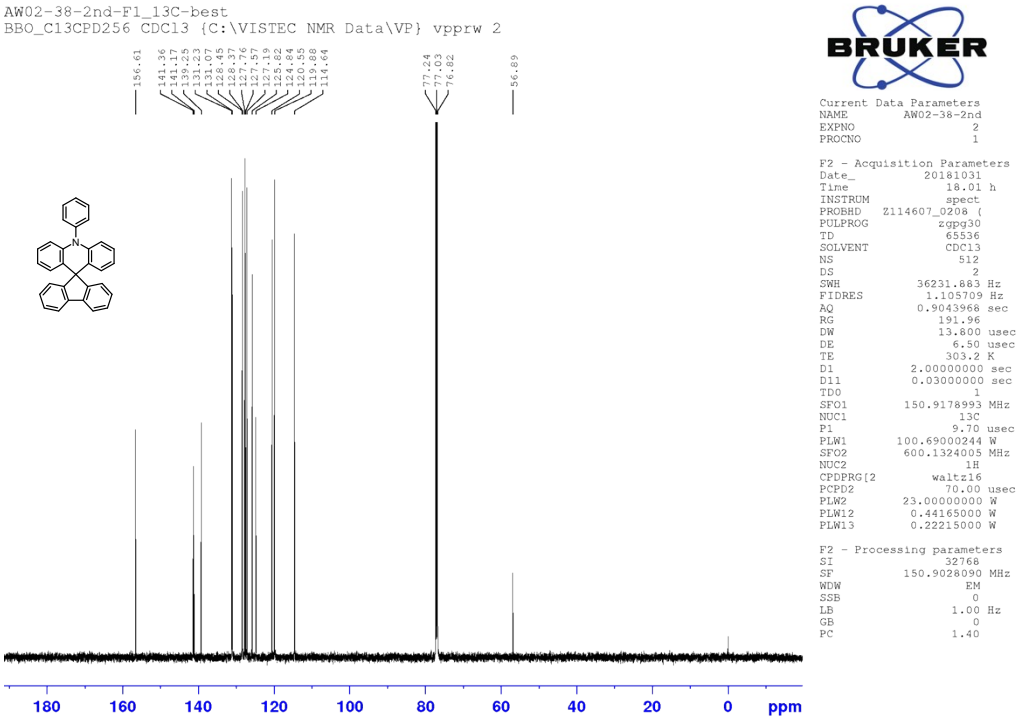


The $^{13}$C NMR spectra of **1** in $CDCl_3$ solution.

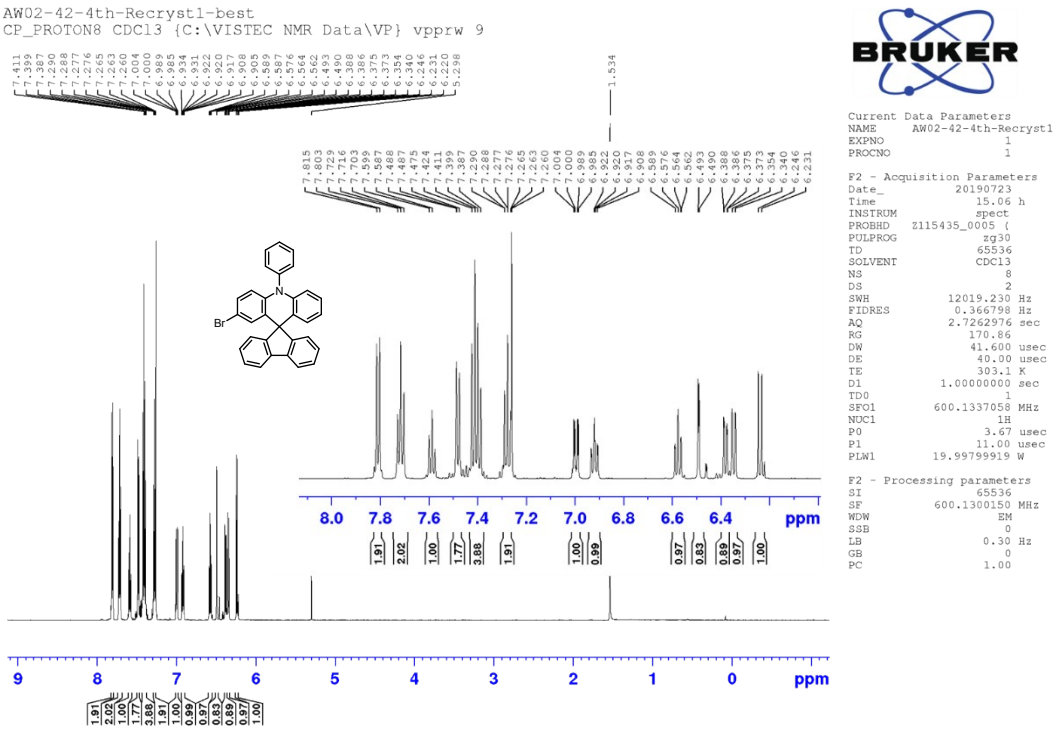


The $^{1}$H NMR spectrum of **2** in $CDCl_3$ solution.

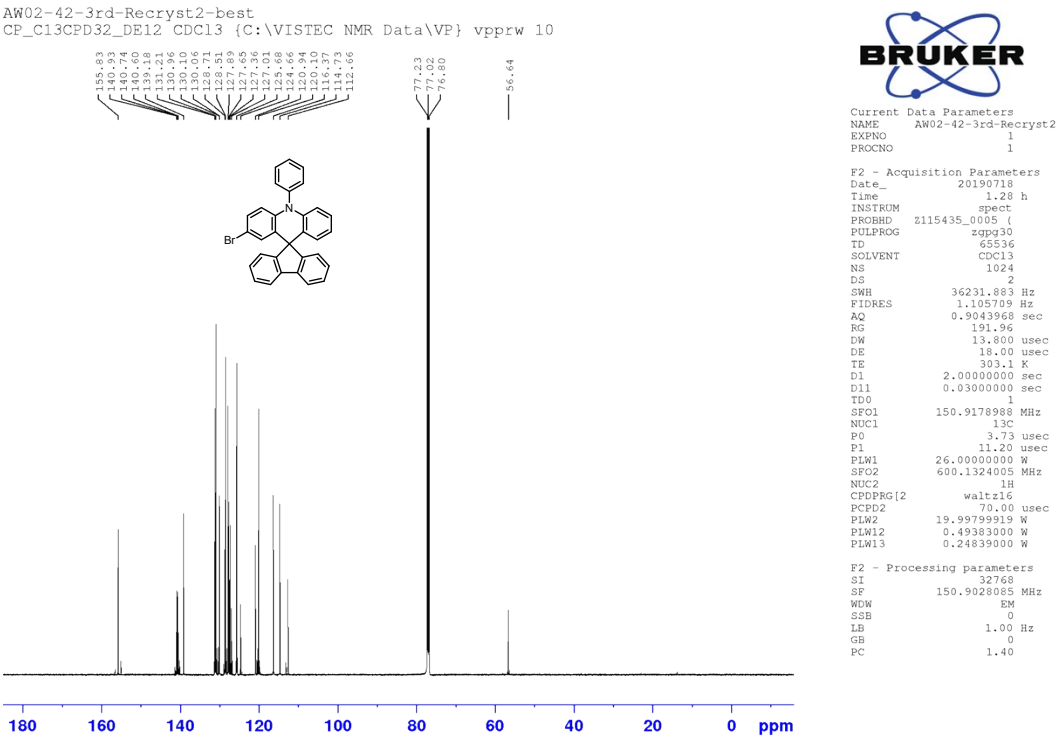


The $^{13}$C NMR spectrum of **2** in $CDCl_3$ solution.

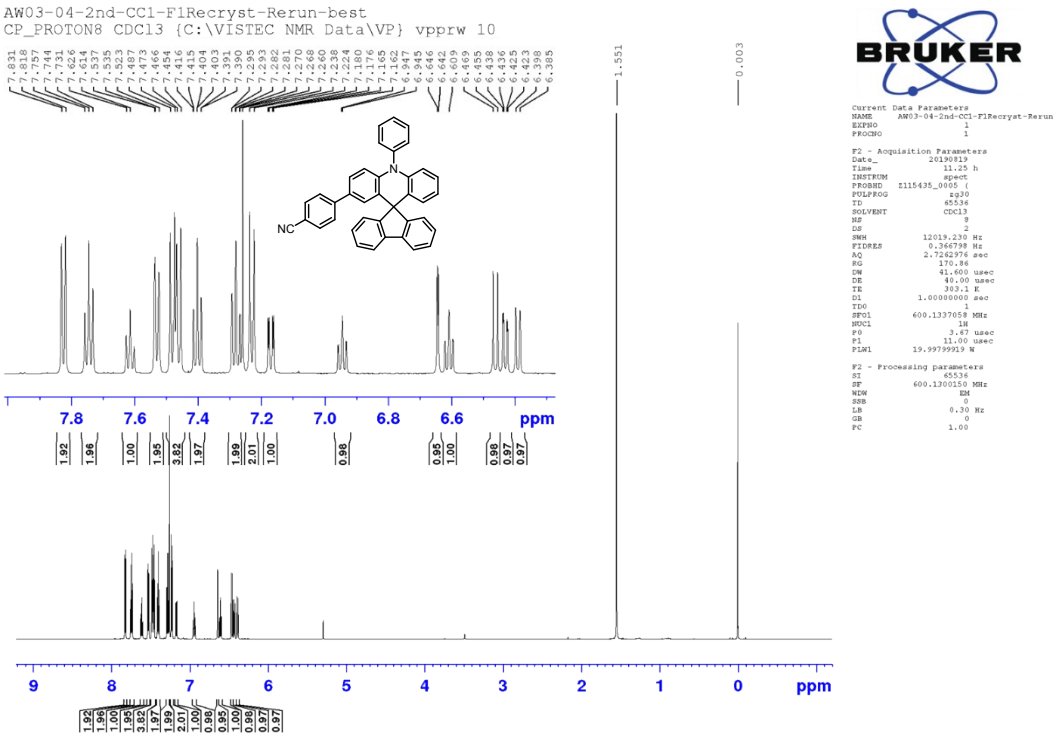


The $^{1}$H NMR spectrum of **SAFpCN** in $CDCl_3$ solution.

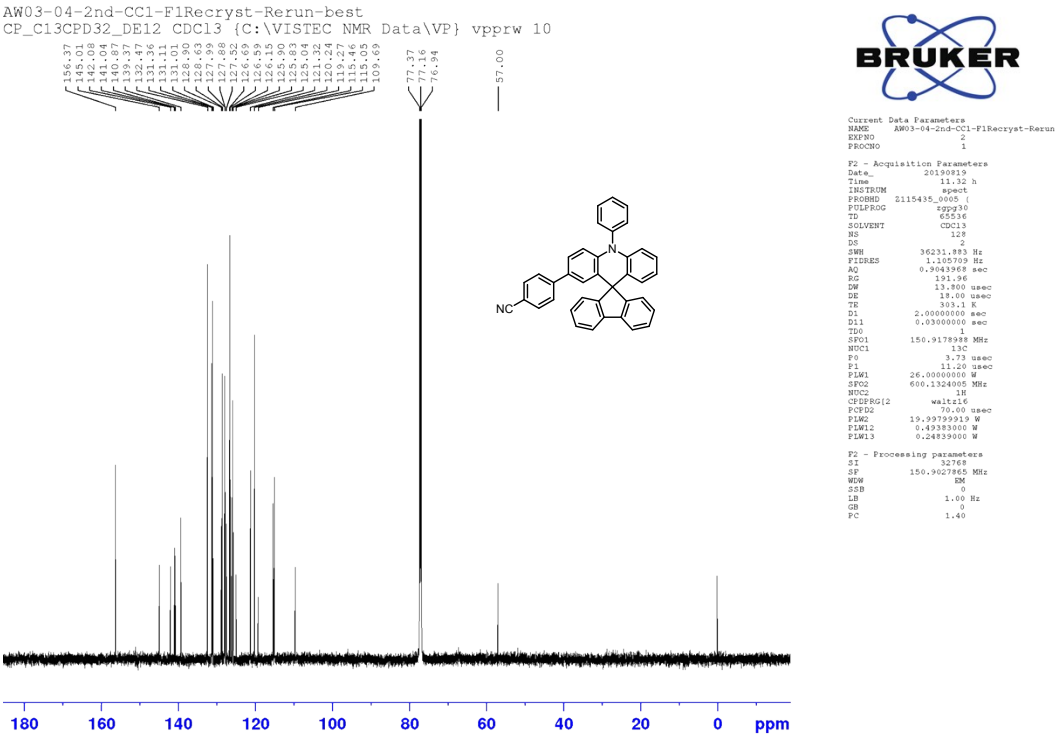


The $^{13}$C NMR spectrum of **SAFpCN** in $CDCl_3$ solution.

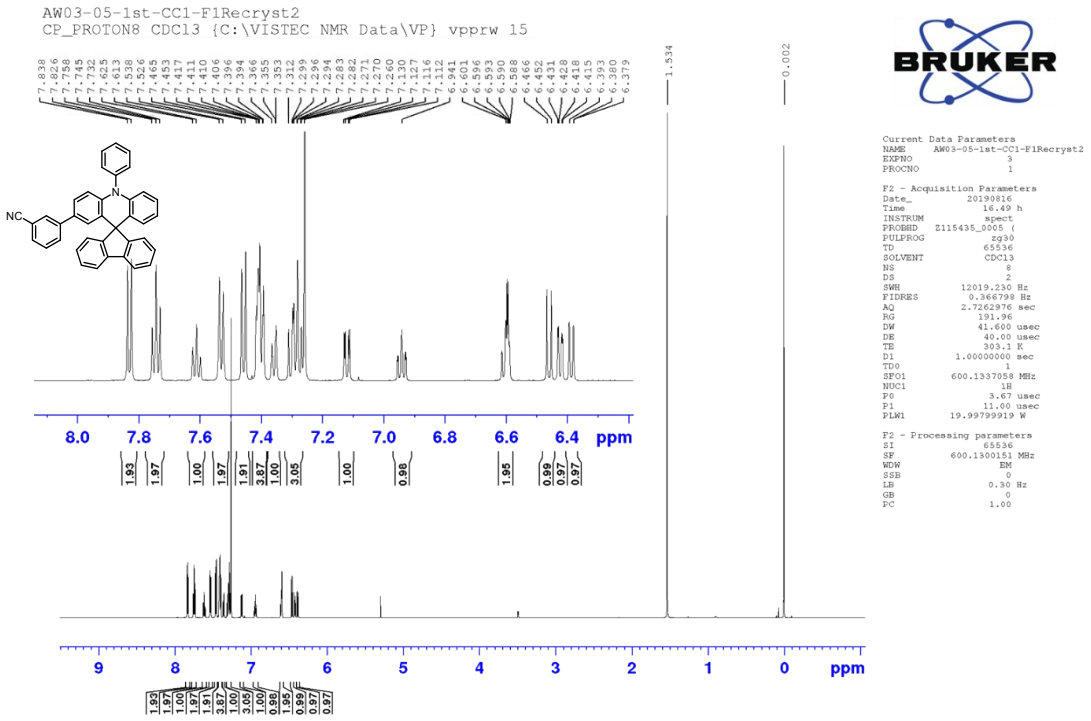


The $^{1}$H NMR spectrum of **SAFmCN** in $CDCl_3$ solution.

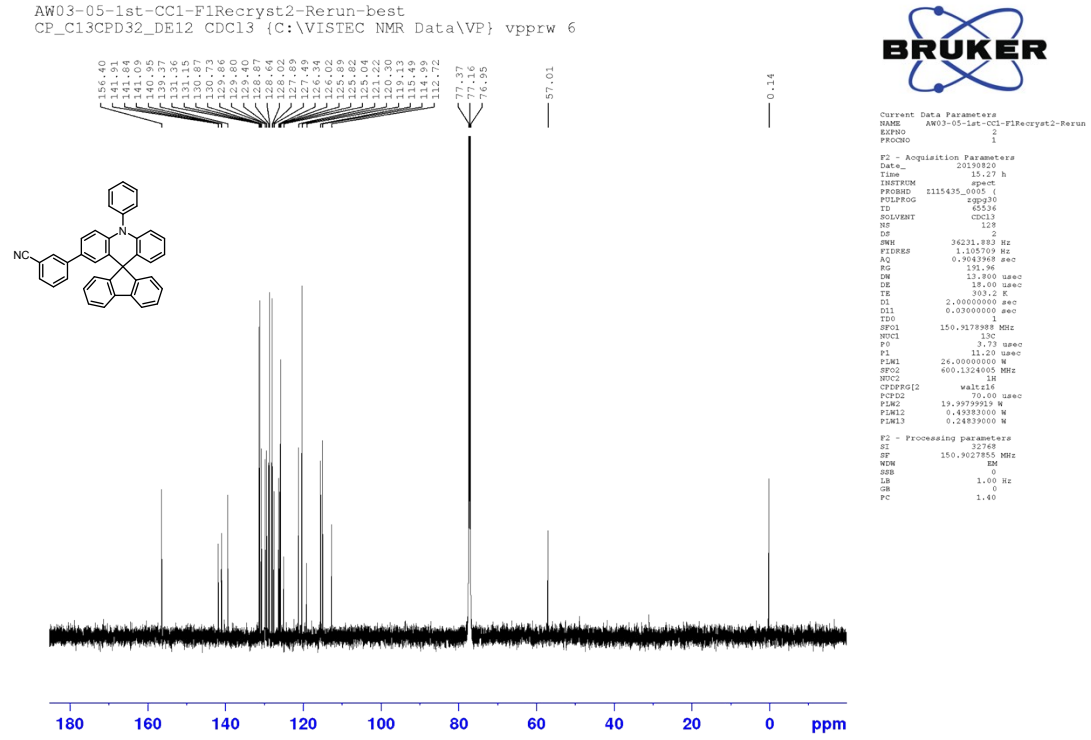


The $^{13}$C NMR spectrum of **SAFmCN** in $CDCl_3$ solution.

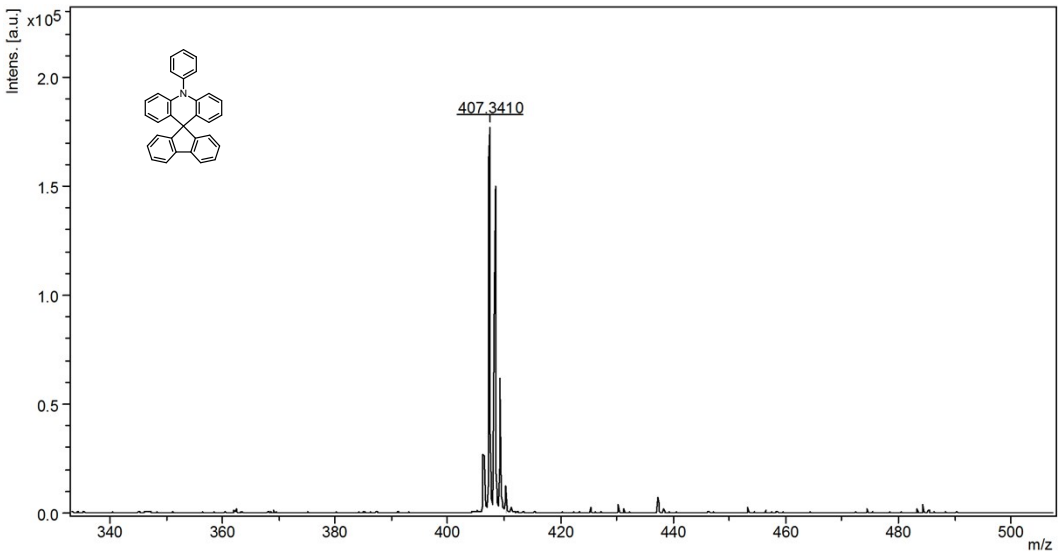


The MALDI-TOF spectra of **1**.

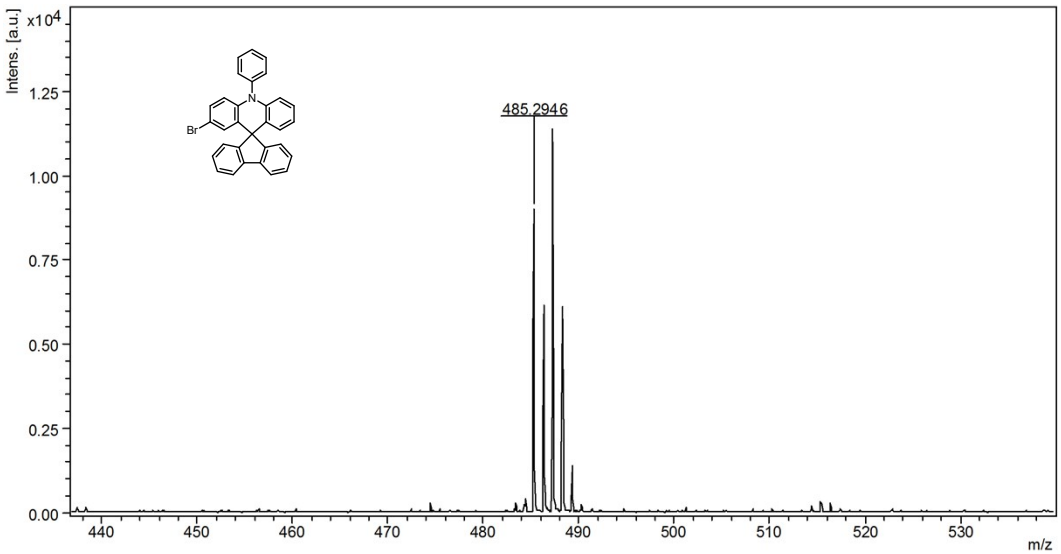


The MALDI-TOF spectrum of **2**.

.

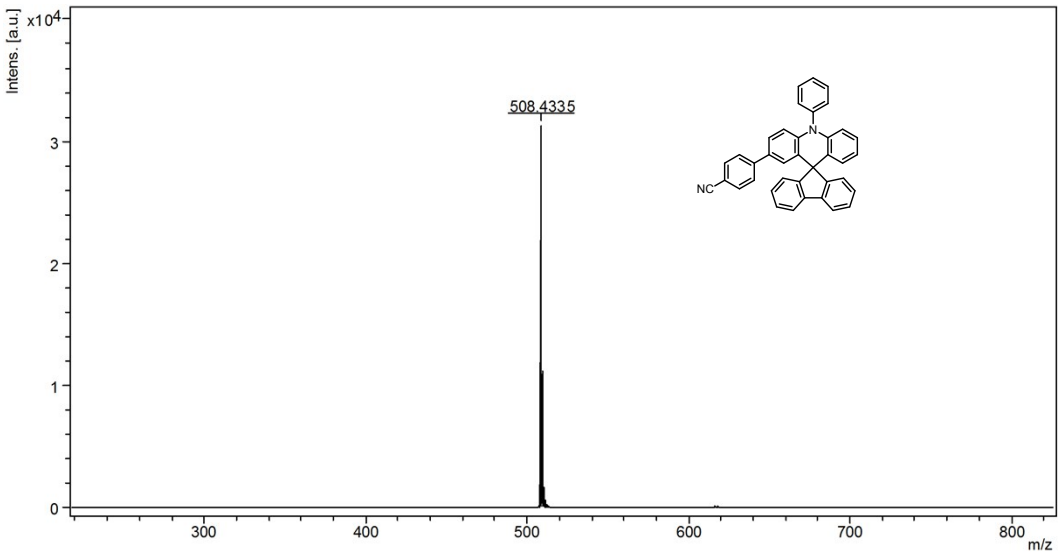


The MALDI-TOF spectrum of **SAFpCN**

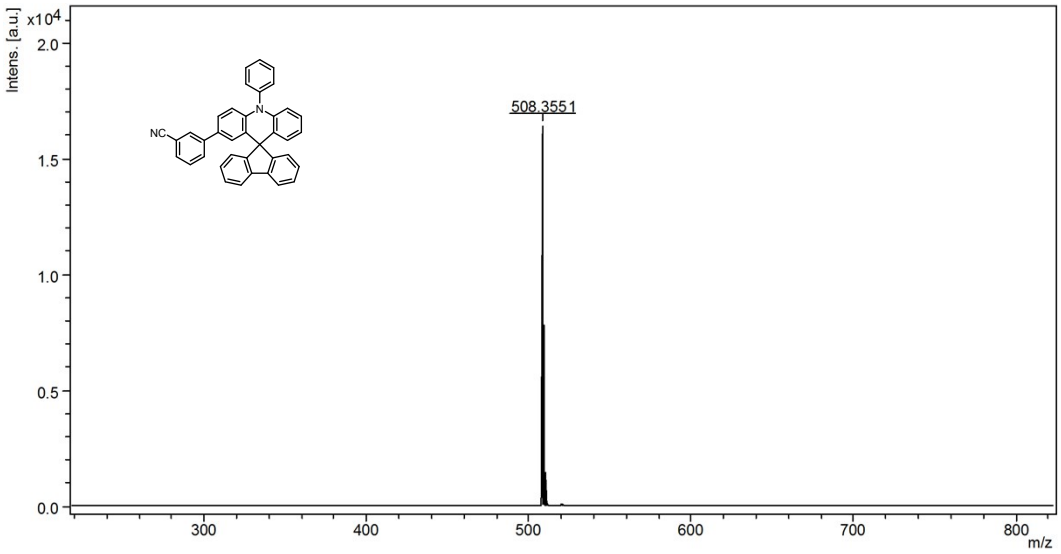


The MALDI-TOF spectrum of **SAFmCN**